New Journal of Physics
The open-access journal for physics

Transport of particles by surface waves: a modification of the classical bouncer model

M Ragulskis[1,3] **and M A F Sanjuán**[2]

[1] Department of Mathematical Research in Systems, Kaunas University of Technology, Studentu 50-222, 51638 Kaunas, Lithuania
[2] Nonlinear Dynamics and Chaos Group, Departamento de Física, Universidad Rey Juan Carlos, Tulipán s/n, 28933 Móstoles, Madrid, Spain
E-mail: minvydas.ragulskis@ktu.lt and miguel.sanjuan@urjc.es

New Journal of Physics **10** (2008) 083017 (9pp)
Received 2 April 2008
Published 14 August 2008
Online at http://www.njp.org/
doi:10.1088/1367-2630/10/8/083017

Abstract. We consider a ball under the influence of gravity on a platform. A propagating surface wave travels on the surface of the platform, while the platform remains motionless. This is a modification of the classical bouncing ball problem and describes the transport of particles by surface waves. Phase and velocity maps cannot be expressed in an explicit form owing to implicit formulations, and no formal analytical analysis is possible. Numerical analysis shows that the transition to chaos is produced via a period doubling route, which is a common property for classical bouncers. The bouncing process can be sensitive to the initial conditions, which can build the ground for control techniques that can dramatically increase the effectiveness of particle transport in practical applications.

Contents

[3] Author to whom any correspondence should be addressed.

1. Introduction

A particle falling down, in a constant gravitational field, on a moving platform is called a bouncing ball problem, or a bouncer. This model was suggested more than 30 years ago [1, 2] as an alternative to the Fermi–Ulam model [3] of cosmic ray acceleration [4]. In the ensuing years, many approaches to the bouncer model have been studied theoretically and experimentally [5]–[8]. It has been proved to be a useful system for experimentally exploring several new nonlinear effects [9, 10]. Moreover, it has been implemented in a number of engineering applications [11, 12].

The bouncer model can be briefly characterized by the following basic statements: (i) maps derived for the bouncer model can be exactly iterated for any time function describing the moving platform [7, 9] (though usually the platform is assumed to oscillate with a single frequency); (ii) the ball platform collisions can be characterized by a coefficient of restitution α changing from $\alpha = 1$ for a perfectly elastic case to $\alpha = 0$ for a completely inelastic situation; and (iii) the chaotic bouncer can be easily used to relate theoretical predictions to experimental results [9, 10], which makes it a paradigm model for the study of nonlinear dynamics.

In this paper, we assume that a particle is falling down in a constant gravitational field on a stationary platform. A propagating surface wave travels on the surface of the platform, while the platform remains motionless. Such a model can be used to describe the transport of particles by propagating surface waves, which is an important problem with numerous applications. Powder transport by piezoelectrically excited ultrasonic surface waves [13], manipulation of bioparticles using traveling wave electrophoresis [14, 15] and conveyance of submerged buoys in coastal waters [16] are just a few examples of problems involving the interaction between propagating waves and transported bouncing particles.

2. The model of the system

Let us consider a two-dimensional system (figure 1): the surface of an elastic plate is represented by a solid line, which coincides with the x-axis in a state of equilibrium. A point on the surface in the state of equilibrium $(x, 0)$ is translated into coordinates (X, Y) when a wave process takes place. This translation is sensitive to time t and coordinate x:

$$\begin{aligned} X &= x + \eta(x, t), \\ Y &= \zeta(x, t), \end{aligned} \tag{1}$$

where the functions $\eta(x, t)$ and $\zeta(x, t)$ determine deflections from the state of equilibrium.

Whenever a traveling non-dispersive Rayleigh surface wave occurs in a medium, it can be characterized by a retrograde elliptic motion of the particles of that medium:

$$\begin{aligned} \eta(x, t) &= a \sin(\omega t - kx), \\ \zeta(x, t) &= b \cos(\omega t - kx), \end{aligned} \tag{2}$$

where a and b are longitudinal and transverse amplitudes of the oscillations; ω is the angular frequency and k is the wave number. Recall that in the usual elastic medium it is quite normal for the transverse displacement to be about 1.5 times larger than the longitudinal displacement [17].

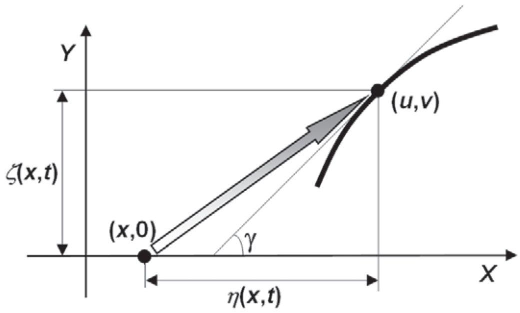

Figure 1. Schematic diagram illustrating the collision between the particle and the surface.

The coordinates of the particle are denoted by (u, v). Assume that the particle is in contact with the surface at time moment t; then the following constraint takes place:

$$v = \zeta(x, t), \tag{3}$$

where x is to be found from the following algebraic equality (where u and t are given and x is the unknown):

$$x + \eta(x, t) = u. \tag{4}$$

In other words, the instantaneous shape of the surface cannot be described by an explicit function. Nevertheless, the tangent to the surface at the point with abscissae u can be expressed explicitly:

$$\tan\gamma = \frac{\partial\zeta(x, t)/\partial x}{1 + \partial\eta(x, t)/\partial x}, \tag{5}$$

where γ is the angle between the tangent and the x-axis. Instantaneous velocities (x- and y-components) of the point on the surface in contact with the particle can be expressed as $\partial\eta(x, t)/\partial t$ and $\partial\zeta(x, t)/\partial t$ accordingly.

The governing equations of motion of a particle in a free flight mode are:

$$\begin{cases} m\ddot{u} + h\dot{u} = 0, \\ m\ddot{v} + h\dot{v} = -mg, \end{cases} \tag{6}$$

where the top dots denote full derivative by time, m is the mass of the particle, h is the coefficient of viscous damping of the media above the surface and g is the free fall acceleration. The initial conditions $u(t_0) = u_0$; $\dot{u}(t_0) = \dot{u}_0$; $v(t_0) = v_0$ and $\dot{v}(t_0) = \dot{v}_0$ yield partial solutions:

$$\begin{aligned} u(t) &= u_0 + \dot{u}_0 \frac{m}{h}\left(1 - \exp\left(-\frac{h}{m}(t - t_0)\right)\right), \\ \dot{u}(t) &= \dot{u}_0 \exp\left(-\frac{h}{m}(t - t_0)\right), \\ v(t) &= v_0 + \left(\dot{v}_0 + \frac{mg}{h}\right)\frac{m}{h}\left(1 - \exp\left(-\frac{h}{m}(t - t_0)\right)\right) - \frac{mg}{h}(t - t_0), \\ \dot{v}(t) &= \dot{v}_0 \exp\left(-\frac{h}{m}(t - t_0)\right) - \frac{mg}{h}\left(1 - \exp\left(-\frac{h}{m}(t - t_0)\right)\right). \end{aligned} \tag{7}$$

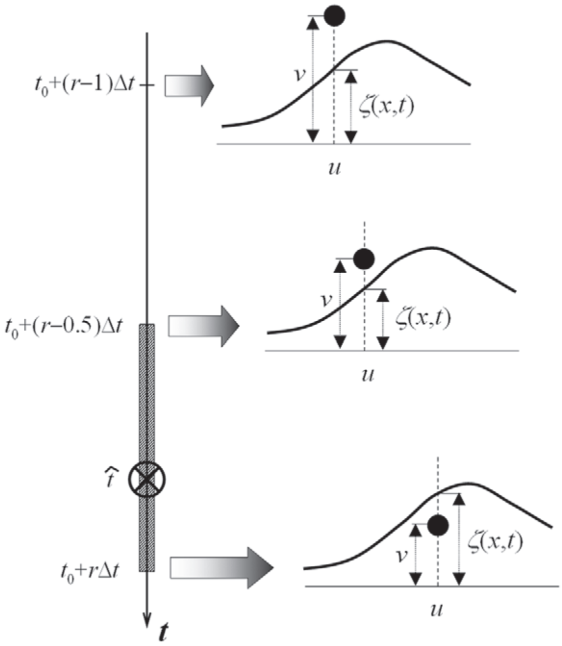

Figure 2. Reconstruction of the collision moment $\hat{t}$. The particle is depicted as a black dot and the surface, as a solid line. Initially, $\hat{t}$ is localized in the rth time interval. Then the bisection rule is used to reach the necessary accuracy. If the particle is in a free flight stage above the surface in the middle of the rth time interval, the search continues in the later subinterval. Note that the instantaneous shape of the surface cannot be expressed explicitly; variables u and x are cross-linked by equation (4).

The free flight stage continues until the particle collides with the surface. Unfortunately, it is impossible to determine the explicit time moment of the collision due to the fact that the instantaneous shape of the surface cannot be expressed by an explicit function. Instead, one has to use iterative numerical techniques in order to determine the exact moment of the bounce.

Localization of the root (the time moment of the collision) is performed using a time marching technique starting from the initial conditions until

$$v(t_0+i\cdot\Delta t) < \zeta(x_i, t_0+i\cdot\Delta t), \tag{8}$$

where Δt is the time step; $i = 1, 2, \ldots, r$; r is the step number for which equation (8) is satisfied for the first time; and x_i is the solution of equation (4) at fixed i:

$$x_i + \eta(x_i, t_0+i\cdot\Delta t) = u(t_0+i\cdot\Delta t); \tag{9}$$

and $u(t_0+i\cdot\Delta t)$ and $v(t_0+i\cdot\Delta t)$ are determined by equation (7). The solution of equation (9) also requires an iterative numerical algorithm.

When the root $\hat{t}$ is localized in the interval $t_0+(r-1)\cdot\Delta t < \hat{t} \leqslant t_0+r\cdot\Delta t$, one needs to determine a more precise estimate of $\hat{t}$ using an iterative computational algorithm (figure 2). This iterative algorithm can be the most simple bisection method, although more sophisticated algorithms comprising the golden section rule or Newton's iterations, for example, can be used instead until the desirable accuracy is achieved. As the collision moment $\hat{t}$ is determined in every iteration, the coordinate $\hat{x}$ (corresponding to the collision point $\hat{u}$: $\hat{x}+\eta(\hat{x},\hat{t})=\hat{u}$) is also made more precise. Initially, $x_{r-1}<\hat{x}\leqslant x_r$; every iteration helps us to reach a better accuracy.

Such an iterative method for the determination of the collision moment leads us to the important conclusion that phase and velocity maps cannot be expressed in an explicit form and no formal analytical analysis is possible.

Nevertheless, the geometrical coordinates of the point of collision are $(\hat{u};\zeta(\hat{x},\hat{t}))$ and can be reconstructed using computational techniques. Velocities of the particle just before the collision are $\dot{u}(\hat{t})$ and $\dot{v}(\hat{t})$. Similarly, instantaneous velocities of the surface in contact with the particle are $\eta_t'(\hat{x},\hat{t})$ and $\zeta_t'(\hat{x},\hat{t})$.

Projections of the particle's velocities just before the collision to the normal and to the tangent to the surface at the contact point can be expressed in the following form:

$$\begin{aligned}\hat{\dot{P}}_n &= -\dot{u}(\hat{t})\sin\gamma+\dot{v}(\hat{t})\cos\gamma,\\ \hat{\dot{P}}_t &= \dot{u}(\hat{t})\cos\gamma+\dot{v}(\hat{t})\sin\gamma,\end{aligned} \tag{10}$$

where the angle γ is determined from equation (5) at the point of collision.

Analogously, projections of velocities of the point on the surface in contact with the particle to the normal and to the tangent take the following form:

$$\begin{aligned}\dot{S}_n &= -\eta_t'(\hat{x},\hat{t})\sin\gamma+\zeta_t'(\hat{x},\hat{t})\cos\gamma,\\ \dot{S}_t &= \eta_t'(\hat{x},\hat{t})\cos\gamma+\zeta_t'(\hat{x},\hat{t})\sin\gamma.\end{aligned} \tag{11}$$

Then, the velocities of the particle just after the collision (in the normal and tangent directions) are:

$$\begin{aligned}\dot{P}_n &= (1+\alpha)\dot{S}_n-\alpha\hat{\dot{P}}_n,\\ \dot{P}_t &= \beta\dot{S}_t+(1-\beta)\hat{\dot{P}}_t,\end{aligned} \tag{12}$$

where α is the coefficient of restitution for the collision in the normal direction. This constant is a measure of the energy loss at each impact. For elastic collisions, $\alpha=1$; for inelastic collisions, $\alpha<1$. The coefficient β determines the friction between the particle and the surface at the moment of collision. There is no friction between the particle and the surface when $\beta=0$. The highest value $\beta=1$ represents the situation when the projection of the particle's velocity (immediately after the impact) and the projection of the surface's point velocity to the tangent are equal.

The free flight stage starts over again immediately after the collision, and the initial conditions are:

$$\begin{aligned}u(\hat{t}) &= \hat{u},\\ \dot{u}(\hat{t}) &= -\dot{P}_n\sin\gamma+\dot{P}_t\cos\gamma,\\ v(\hat{t}) &= \zeta(\hat{x},\hat{t}),\\ \dot{v}(\hat{t}) &= \dot{P}_n\cos\gamma+\dot{P}_t\sin\gamma.\end{aligned} \tag{13}$$

The presented model is a modification of the classic bouncer model which can be derived assuming $\zeta(x,t)=b\cos(\omega t)$ and $\eta(x,t)=0$. In that case, $u=x$ and the model becomes explicit.

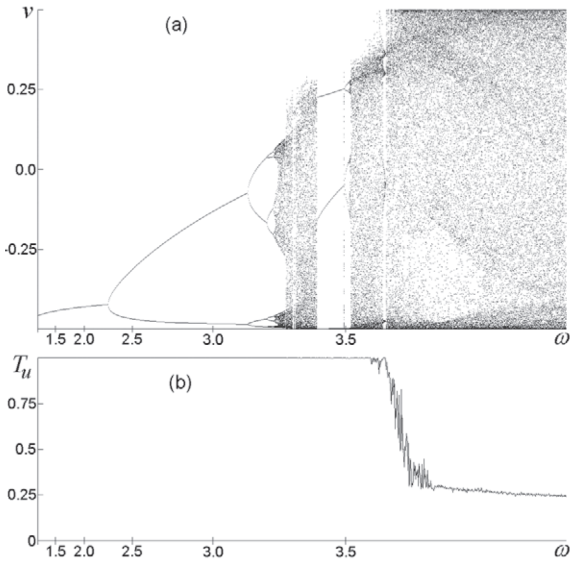

Figure 3. Transport of particles at increasing wave speeds (elastic collisions, viscous medium over the surface). Reduced impact representation (a) shows the transition to chaos via a period doubling route. Note that impact heights are distributed in the interval $[-0.5, 0.5]$. The non-dimensional longitudinal particle's transport velocity T_u drops down at higher wave speeds due to the viscosity of the medium above the surface (b). The system's parameters are: $\alpha = 1$; $\beta = 0$; $\eta(x, t) = \frac{2}{3}\sin(\omega t - x)$; $\zeta(x, t) = \frac{1}{2}\cos(\omega t - x)$; $h = 0.1$; $m = 0.5$; and $g = 9.81$.

3. Nonlinear dynamics of the modified bouncer

We will demonstrate that the modified bouncer model possesses such an inherent feature as chaotic dynamics. Moreover, we will show that the sensitivity to initial conditions can be exploited for the control of the process of conveyance.

Initially, we will assume that collisions are completely elastic ($\alpha = 1$) and there is no tangential friction between the particle and the surface ($\beta = 0$), but the medium above the surface is viscous ($h = 0.1$). We use the reduced impact representation, where the height of the bouncing ball is sampled at each impact with the surface (impact sampling). Since the system is dissipative, we plot the bouncing process after the initial transients cease down (figure 3(a)). We skip 1500 successive bounces before starting to plot the collision heights $v(\hat{t})$ for every discrete value of ω. The parameter ω is varied following the rule $\omega_i = 1 + (3/\ln 21)\ln(1 + (20i/1024))$; $i = 1, \ldots, 1024$, which helps us to expand the cascade of period doubling bifurcations. The control parameter in our case is not the amplitude of the platform's oscillation but the velocity of the wave propagation; the collision height is used instead of collision velocity for a reduced impact representation. Moreover, the medium above the surface of the plate is viscous. It appears that the transition to chaos via a period doubling route observed for a classical bouncer [18] is observed also for a particle bouncing on the surface of a stationary platform with a propagating wave traveling on its surface.

A phenomenological model could be used to exemplify the bifurcation diagram presented in figure 3(a). The logistic map [19] is probably the simplest model ever used to study

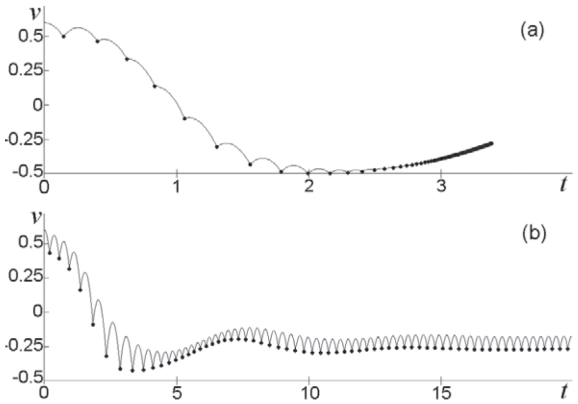

Figure 4. Sensitivity of transient processes to initial conditions. The particle's trajectories are plotted as solid lines and collision heights as solid dots. The system's parameters are: $\alpha = 0.82$, $\beta = 0.02$, $\eta(x, t) = \frac{2}{3}\sin(t - x)$, $\zeta(x, t) = \frac{1}{2}\cos(t - x)$, $h = 0.1$, $m = 0.5$ and $g = 9.81$. The initial conditions $u(0) = 0$, $\dot{u}(0) = 1$, $v(0) = 0.6$ and $\dot{v}(0) = 0$ result in complete chattering (a), whereas $u(0) = 0$, $\dot{u}(0) = 2$; $v(0) = 0.6$ and $\dot{v}(0) = 0$ result in infinite bouncing (b). Note the different timescales in (a) and (b).

the transition to chaos via a period doubling route. Simple computational experiments with appropriately chosen parameter values of the logistic map would illustrate the universality of the bifurcation diagram shown in figure 3(a).

An important parameter characterizing the effectiveness of the transport is the average longitudinal velocity of the particle $\bar{\dot{u}}$. We average it over a long period of time after the initial transients cease down. In order to calculate a non-dimensional quantity, we divide the average longitudinal velocity by the velocity of the traveling wave $T_u = k\bar{\dot{u}}/\omega$. Thus, the average velocity of conveyance is equal to the velocity of the traveling wave when T_u is equal to 1 (figure 3(b)).

It is interesting to observe that the particle is transported with the average velocity of the traveling wave until the period 3 bouncing mode after a cascade of period doubling bifurcations (figure 3(a)). The particle's average transportation velocity drops down only when the period 3 bouncing mode experiences its own cascade of period doubling bifurcations. External damping forces acting on the particle prevent its motion with the average wave's velocity in the direction of the wave propagation when this velocity becomes large enough (even though the collisions are elastic). Also, the bouncing process is insensitive to initial conditions—eventually it converges to the one and only attractor shown in figure 3(a) (at fixed ω).

The situation becomes different when collisions are inelastic. Figure 4(a) illustrates a vanishing bouncing process (complete chattering [18]) when the particle sets into the state of rest on a slope of the propagating wave. The term 'complete chattering' is used in the literature to describe the process when the time interval between inelastic bounces tends to zero and the ball finally 'sticks' to the surface of the oscillating platform. It can be noted that the collision heights are plotted versus time t, not coordinate u in figure 4(a). The time interval between adjacent collisions converges to zero (figure 4(a)) until the bouncing particle model becomes inadequate and the dynamics of the system must be analyzed exploiting a sliding particle model.

The sliding particle model on the surface of a propagating wave (the detailed description of this model is given in [20]) can exhibit a rich dynamic behavior characterized by coexisting attractors. One of these attractors is a stable equilibrium point. It corresponds to a steady sliding motion on one slope of the propagating wave. Another attractor is a stable limit cycle. It corresponds to an oscillatory motion with a small average velocity compared with the wave's propagation velocity; the particle slides over the peaks of the wave. The characteristic shape of the basin boundaries of coexisting attractors [20] can be exploited for the development of attractor control techniques. These techniques are based on small external impulses [21] and can dramatically increase the effectiveness of the conveyance. The trajectory of the limit cycle is located quite near the basin boundary, so that a small single external force impulse can kick the trajectory from the limit cycle to the basin of the equilibrium point (the reverse is not so simple). It is quite natural to expect that the bouncing particle model should also exhibit the sensitivity to initial conditions at certain sets of system parameters. In fact figure 4(b) illustrates this effect. All system parameters in figures 4(a) and (b) are the same except for the initial velocity $\dot{u}(0)$. The bouncing process terminates into the sliding mode in figure 4(a), whereas it continues infinitely in figure 4(b).

4. Concluding remarks

Transport of particles by surface waves is an important scientific and engineering problem, with numerous practical applications, including micro-electro-mechanical systems (MEMS), used to manipulate objects like particles or cells. We show that this problem is a modification of the classical bouncer model, which is considered as a paradigm model in nonlinear physics. The formulations of our model are implicit, thus phase and velocity maps cannot be expressed in an explicit form.

Chaotic dynamics of a conveyed particle is not an unexpected fact due to the complexity of the constitutive model. More surprising is the rich dynamical behavior in models comprising dissipative dynamics, elastic and inelastic collisions. It appears that the transition to chaos via a period doubling route is a universal property for bouncers and is observed in our model of particle transport in viscous media. It is also shown how the bouncing ball problem is transformed into a sliding ball problem. Moreover, the sensitivity to initial conditions can build the ground for control techniques which can dramatically increase the effectiveness of the particles' transport by surface waves.

Although the numerical analysis was concentrated on the dimensionless system only, theoretical and experimental investigation of dry particle conveyance and its control is a suitable object for future research.

Acknowledgment

Financial support from the Spanish Ministry of Education and Science under project number FIS2006-08525 is acknowledged.

References

[1] Zaslavsky G M 1978 *Phys. Lett.* A **69** 145
[2] Pustilnikov L D 1983 *Theor. Math. Phys.* **57** 1035
[3] Lieberman M A and Lichtenberg A J 1971 *Phys. Rev.* A **5** 1852

[4] Fermi E 1949 *Phys. Rev.* **75** 1169
[5] Chirikov B V 1979 *Phys. Rev.* **52** 263
[6] Lichtenberg A J, Lieberman M A and Cohen R H 1980 *Physica* D **1** 291
[7] Pieranski P and Malecki J 1986 *Phys. Rev.* A **34** 582
[8] Everson R M 1986 *Physica* D **19** 355
[9] Wiesenfeld K and Tuffilaro N B 1987 *Physica* D **26** 321
[10] Kowalik Z J, Franaszek M and Pieranski P 1988 *Phys. Rev.* A **37** 4016
[11] Hongler M O, Cartier P and Flury P 1989 *Phys. Lett.* A **135** 106
[12] Hongler M O and Figour J 1989 *Helv. Phys. Acta* **62** 68
[13] Mracek M and Wallaschek J 2005 *Mater. Chem. Phys.* **90** 378
[14] Talary M S, Burt J P H, Tame J A and Pethig R 1996 *J. Phys. D: Appl. Phys.* **29** 2198
[15] Chou C F, Tegenfeldt J O, Bakajin O, Chan S S, Cox E C, Darnton N, Duke T and Austin R H 2002 *Biophys. J.* **83** 2170
[16] Plaut R H, Farmer A L and Holland M M 2001 *J. Vib. Acoust.* **123** 333
[17] Landau L D and Lifschitz E M 1986 *Theory of Elasticity* (Oxford: Pergamon) p 187
[18] Luck J M and Mehta A 1993 *Phys. Rev.* E **48** 3988
[19] May R M 1976 *Nature* **261** 459
[20] Ragulskis M and Koizumi K 2004 *J. Vib. Control* **10** 1057
[21] Ragulskis M 2004 *J. Vib. Control* **10** 101